# Correspondence

## On Accuracy of Virtual Signal Injection based MTPA Operation of Interior Permanent Magnet Synchronous Machine Drives

Tianfu Sun, Jiabin Wang, and Mikail Koc

***Abstract*—This correspondence analyzes the accuracy of maximum torque per ampere (MTPA) operations of interior permanent magnet machines based on the technique described in [T. Sun, J. Wang, and X. Chen, "Maximum Torque Per Ampere (MTPA) Control for Interior Permanent Magnet Synchronous Machine Drives Based on Virtual Signal Injection," IEEE Trans. Power Electron., vol. 30, no. 9, pp. 5036-5045, Sep. 2015] in responses to a few inquiries made by the readers. It is shown that due to parameter variations with stator currents, any technique for MTPA tracking based on piecewise constant parameter assumption, i.e., the machine parameters are assumed as constants during the calculation of $\partial T_e/\partial\beta$, would result in tracking error even though the machine parameters are obtained from lookup table or online machine parameter estimations. The error is dependent on machine nonlinear characteristics and operating conditions. It is also shown that for the prototype interior permanent magnet synchronous machine the virtual signal injection control technique described in the paper mentioned above yields a better tracking accuracy.**

***Index Terms*—Interior permanent magnet synchronous machine (IPMSM) drives, maximum torque per ampere (MTPA), signal injection, virtual signal injection control (VSIC).**

### I. Introduction

Since the publication of the paper titled "Maximum Torque Per Ampere (MTPA) Control for Interior Permanent Magnet Synchronous Machine Drives Based on Virtual Signal Injection," we have received a few inquiries from readers with regard to MTPA tracking accuracy of the proposed technique. Rigorous analysis supported by extensive simulations and experiments have been made, and our findings are described in this letter.

The mathematical model of an interior permanent magnet synchronous machine (IPMSM) in the *d–q* reference frame neglecting high-order space harmonics is given by

$$v_q = L_q\frac{di_q}{dt} + Ri_q + p\omega_m L_d i_d + p\omega_m \Psi_m \tag{1}$$

$$v_d = L_d\frac{di_d}{dt} + Ri_d - p\omega_m L_q i_q \tag{2}$$

$$T_e = \frac{3p}{2}\left[\Psi_m i_q + (L_d - L_q) i_d i_q\right] \tag{3}$$

$$i_d = -I_a \sin(\beta) \tag{4}$$

$$i_q = I_a \cos(\beta) \tag{5}$$

Manuscript received August 27, 2016; revised October 22, 2016; accepted November 28, 2016. Date of publication December 9, 2016; date of current version April 24, 2017. Recommended for publication by Associate Editor B. Wang.

The authors are with the Department of Electronic and Electrical Engineering, The University of Sheffield, Sheffield S1 3JD, U.K. (e-mail: tianfu.sun@foxmail.com; j.b.wang@sheffield.ac.uk; mikaelkoc@gmail.com).

Color versions of one or more of the figures in this paper are available online at http://ieeexplore.ieee.org.

Digital Object Identifier 10.1109/TPEL.2016.2638020

where $v_d, v_q$ are the *d*- and *q*-axis stator voltages; $i_d,\ i_q, I_a$ are the *d*- and *q*-axis stator currents and the current vector amplitude; *R* is the stator phase resistance; $L_d, L_q$ are the *d*- and *q*-axes inductances; $T_e$ is the electromagnetic torque; *p* is the number of pole pairs of the motor; $\omega_m$ is the rotor angular speed in rad/s; $\Psi_m$ is the flux linkage due to permanent magnet excitation; and $\beta$ is the current angle between the current vector and the *q*-axis, also known as leading angle.

In most IPMSM machines, $\Psi_m$, $L_d$ and $L_q$ are dependent on the stator currents due to the magnetic saturation. According to (1) and (2), the following relations can be derived in steady state:

$$\Psi_m = \Psi_d - L_d i_d = \frac{v_q - Ri_q}{p\omega_m} - L_d i_d \tag{6}$$

$$(L_d - L_q) = \frac{v_d - Ri_d}{p\omega_m i_q} + L_d \tag{7}$$

where $\Psi_d$ is the *d*-axis flux linkage of the machine. Substituting (6) and (7) into (3) leads to

$$T_{e\_1} = \frac{3p}{2}\left\{\left(\frac{v_q - Ri_q}{p\omega_m} - L_d i_d\right) + \left(L_d + \frac{v_d - Ri_d}{p\omega_m i_q}\right) i_d\right\} i_q. \tag{8}$$

The significance of the expression in (8) is that only $L_d$ is required for torque evaluation. If a small high-frequency sinusoidal signal $\Delta\beta$ is injected into the stator current angle $\beta$ according to (4) and (5), the corresponding *d*- and *q*-axis currents $i_d^h$ and $i_q^h$ can be expressed in (10) and (11), respectively,

$$\Delta\beta = A\sin(\omega_h t) \tag{9}$$

$$i_d^h = -I_a \sin(\beta + \Delta\beta) \tag{10}$$

$$i_q^h = I_a \cos(\beta + \Delta\beta) \tag{11}$$

where $\omega_h$ is the angular frequency of the injected signal. If the machine parameters are assumed to be piecewise constant and varies with operation conditions, the relationship between the torque and *d*- and *q*-axis currents can be approximated by a polynomial in the form of (12), where $a$ and $b$ given in (13) and (14) and are assumed to be piecewise constant and varies with operation conditions

$$T_{e\_1} = \frac{3p}{2}(a + bi_d) i_q \tag{12}$$

$$a = \Psi_m = \frac{v_q - Ri_q}{p\omega_m} - L_d i_d \tag{13}$$

$$b = (L_d - L_q) = \frac{v_d - Ri_d}{p\omega_m i_q} + L_d. \tag{14}$$

Substituting (10) and (11) into (12) yields

$$T_{e\_1}^h = \frac{3p}{2}\left\{\frac{v_q - Ri_q}{p\omega_m} - L_d\left(i_d - i_d^h\right) + \frac{v_d - Ri_d}{p\omega_m i_q} i_d^h\right\} i_q^h. \tag{15}$$

Since $L_d$ in IPMSMs is always the smallest machine parameter, which is much smaller than $L_q$ and $\Psi_m$, $L_d$ can be obtained from look-up table or assumed to its nominal value. If $L_d(i_d - i_d^h)$ is ignored, (15) is simplified to (16) and the corresponding calculated electromagnetic torque without high-frequency components is given by (17). The significance of the expression in (16) and (17) is that it does not contain machine parameters. The errors of virtual signal injection based on (15) and (16) will be discussed and compared below

$$T_{e\_2}^h = \frac{3p}{2}\left[\frac{(v_q - Ri_q)}{\omega_m} + \frac{(v_d - Ri_d)}{i_q\omega_m} i_d^h\right] i_q^h = \frac{3p}{2}\left[m + ni_d^h\right] i_q^h \tag{16}$$

$$T_{e\_2} = \frac{3p}{2}\left[\frac{(v_q - Ri_q)}{\omega_m} + \frac{(v_d - Ri_d)}{i_q\omega_m} i_d\right] i_q = \frac{3p}{2}\left[m + ni_d\right] i_q \tag{17}$$

$$m = \frac{(v_q - Ri_q)}{\omega_m} = \Psi_d \tag{18}$$

$$n = \frac{(v_d - Ri_d)}{i_q\omega_m} = -L_q. \tag{19}$$

The signal processing of the virtual signal injection for MTPA tracking described in [1] is based on (16). It essentially tracks $\partial T_{e\_2}/\partial\beta = 0$ for a given operating point. If *a*, *b*, *m,* and *n* are assumed to be piecewise constant, depending on operation conditions, their derivatives with respect to the current angle $\beta$ are zero. The torque derivatives of (12) and (17) with respect to $\beta$ can be expressed in (20) and (21), respectively. Similarly, if $T_{e\_1}^h$ in (15) is employed by the same signal processing scheme described in [1], the output of the signal processing block will be proportional to $\partial T_{e\_1}/\partial\beta$ given in (20) and the scheme will track $\partial T_{e\_1}/\partial\beta = 0$, which is equivalent to the conventional methods in [3]–[9] but only the $L_d$ is needed

$$\frac{\partial T_{e\_1}}{\partial\beta} = \frac{3p}{2}\left[-aI_a\sin\beta - bI_a^2\cos 2\beta\right] \tag{20}$$

$$\frac{\partial T_{e\_2}}{\partial\beta} = \frac{3p}{2}\left[-mI_a\sin\beta - nI_a^2\cos 2\beta\right]. \tag{21}$$

Substituting (13) and (14) into (20) leads to

$$\frac{\partial T_{e\_1}}{\partial\beta} = \frac{3p}{2}\left[-\Psi_m I_a\sin\beta - L_d I_a^2\cos 2\beta + L_q I_a^2\cos 2\beta\right]. \tag{22}$$

Substituting (18) and (19) into (21) gives

$$\frac{\partial T_{e\_2}}{\partial\beta} = \frac{3p}{2}\left[-\Psi_d I_a\sin\beta + L_q I_a^2\cos 2\beta\right]. \tag{23}$$

It is worth noting that (22) and (23) are also applicable when accurate machine parameters are obtained from look-up tables or online parameter estimations. However, if the machine parameter variations with the current angle are fully considered, i.e., consider the terms $\partial\Psi_m/\partial\beta$, $\partial L_d/\partial\beta$, and $\partial L_q/\partial\beta$, according to (3), the actual torque derivative with respect to the current angle should be expressed in the following equation:

$$\frac{\partial T_e}{\partial\beta} = \frac{3p}{2}\left\{-\Psi_m I_a\sin\beta + \frac{\partial\Psi_m}{\partial\beta} I_a\cos\beta - L_d I_a^2\cos 2\beta + L_q I_a^2\cos 2\beta - \frac{\partial L_d}{\partial\beta}\frac{I_a^2}{2}\sin 2\beta + \frac{\partial L_q}{\partial\beta}\frac{I_a^2}{2}\sin 2\beta\right\}. \tag{24}$$

Comparison of (22) with (24) yields

$$\frac{\partial T_{e\_1}}{\partial\beta} = \frac{\partial T_e}{\partial\beta} - error_1. \tag{25}$$

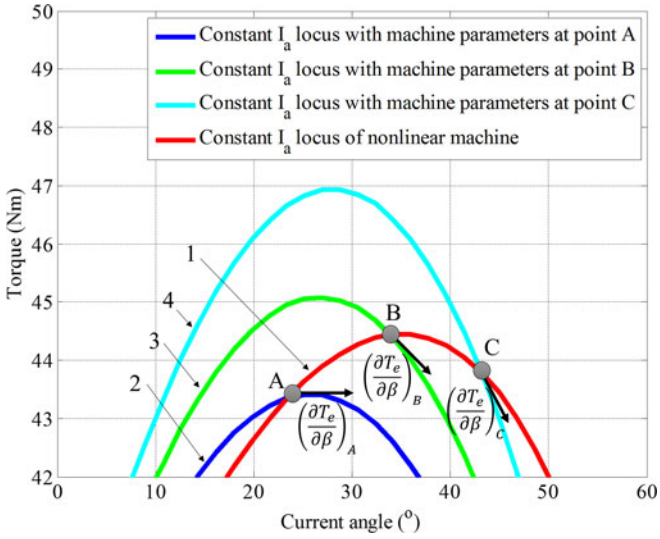


Fig. 1. Torque variations with $\beta$ obtained from different machine parameters and nonlinear machine model when $I_a = 77$ A.

Comparison of (23) with (24) leads to

$$\frac{\partial T_{e\_2}}{\partial\beta} = \frac{\partial T_e}{\partial\beta} - error_2 \tag{26}$$

where

$$error_1 = \frac{3p}{2}\left[\frac{\partial\Psi_m}{\partial\beta} + \frac{\partial L_d}{\partial\beta} i_d - \frac{\partial L_q}{\partial\beta} i_d\right] i_q \tag{27}$$

$$error_2 = \frac{3p}{2}\left[\frac{\partial\Psi_m}{\partial\beta} + \frac{\partial L_d}{\partial\beta} i_d - \frac{\partial L_q}{\partial\beta} i_d - L_d i_q\right] i_q. \tag{28}$$

As can be seen from (27) and (28), use of accurate machine parameters to calculate the MTPA points by letting $\partial T_{e\_1}/\partial\beta = 0$ or $\partial T_{e\_2}/\partial\beta = 0$ will still incur inevitable error if these parameters are assumed to be piecewise constants.

In order to verify the above analysis, simulations were first performed based on the nonlinear IPMSM model adopted in [1] and the resultant torque variation with torque angle $\beta$ for a given current amplitude of 77 A is designated as locus 1, as shown in in Fig. 1. The machine parameters ($\Psi_m$, $L_d$, $L_q$) at points A, B, and C on locus 1 are also recorded. Simulations were then performed based on (3) with the machine parameters at points A, B, and C, respectively. The resultant torque variations with $\beta$ for the same current amplitude are denoted as locus 2, 3, and 4, respectively. As can be seen from Fig. 1, the derivatives $\partial T_e/\partial\beta$ obtained from the nonlinear parameter model at points A, B, and C are always greater than $(\partial T_e/\partial\beta)_A$, $(\partial T_e/\partial\beta)_B$, and $(\partial T_e/\partial\beta)_C$, which are obtained assuming constant parameters at these points. This is due to the fact that $error_1 > 0$. Moreover, the torque variation with $\beta$ of the nonlinear machine model in the vicinity of the MTPA point is flatter than those of loci 2, 3, and 4 around their MTPA points. The machine parameter variations with $\beta$ cause the true MTPA point to shift toward the right.

The implication of the foregoing analysis must be appreciated. First, for IPMSMs with constant parameters, the MTPA tracking error based on (15) will be zero. This condition is unlikely to be true in practical IPMSM machines due to magnetic saturation. However, numerous papers reported in literature derived MTPA or minimum power loss conditions based on the piecewise constant parameter assumptions [without taking account of the $\partial\Psi_m/\partial\beta$, $\partial L_d/\partial\beta$, and $\partial L_q/\partial\beta$ in (24)]. These include online calculation of MTPA reference current

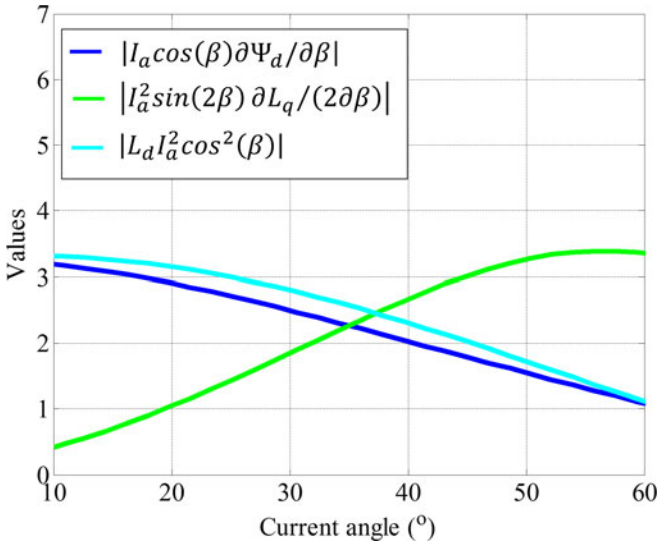


Fig. 2. Variations of $|I_a^2 \sin 2\beta\partial L_q/(2\partial\beta)|$, $|L_d I_a^2 \cos^2(\beta)|$ and $|I_a \cos(\beta)\partial\Psi_d/\partial\beta|$ with $\beta$ when $I_a = 77$ A.

commands based on parameter look-up tables through Lagrange multiplier method [2], Newton's method [3], or through Ferrari's method [4], and based on online parameter estimations [5]–[9]. They will not yield accurate MTPA operations if parameter variations with the stator currents are significant. For example, point B in Fig. 1 is very close to the true MTPA point. However, the MTPA point obtained by assuming piecewise constant machine parameters at this point is close to point A, and deviates significantly from the true MTPA operation.

Since

$$\frac{\partial\Psi_d}{\partial\beta} = \frac{\partial\Psi_m}{\partial\beta} + \frac{\partial L_d}{\partial\beta} i_d - L_d i_q \tag{29}$$

(27) and (28) can be further expressed as

$$error_1 = \frac{3p}{2}\left[\frac{\partial\Psi_d}{\partial\beta} i_q - \frac{\partial L_q}{\partial\beta} i_d i_q + L_d i_q^2\right] \tag{30}$$

$$error_2 = \frac{3p}{2}\left[\frac{\partial\Psi_d}{\partial\beta} i_q - \frac{\partial L_q}{\partial\beta} i_d i_q\right]. \tag{31}$$

Since for both motoring operations and generating operations $i_q\partial\Psi_d/\partial\beta$ and $i_d i_q \partial L_q/\partial\beta$ are negative and $L_d i_q^2$ is positive, (30) and (31) can be written as (32) and (33)

$$\begin{aligned} error_1 &= \frac{3p}{2}\left[\left|\frac{\partial L_q}{\partial\beta} i_d i_q\right| + \left|L_d i_q^2\right| - \left|\frac{\partial\Psi_d}{\partial\beta} i_q\right|\right] \\ &= \frac{3p}{2}\left[\left|\frac{\partial L_q}{\partial\beta}\frac{I_a^2 \sin 2\beta}{2}\right| + \left|L_d I_a^2 cos^2(\beta)\right| \right. \\ &\quad \left. - \left|\frac{\partial\Psi_d}{\partial\beta} I_a \cos(\beta)\right|\right] \end{aligned} \tag{32}$$

$$\begin{aligned} error_2 &= \frac{3p}{2}\left[\left|\frac{\partial L_q}{\partial\beta} i_d i_q\right| - \left|\frac{\partial\Psi_d}{\partial\beta} i_q\right|\right] \\ &= \frac{3p}{2}\left[\left|\frac{\partial L_q}{\partial\beta}\frac{I_a^2 \sin 2\beta}{2}\right| - \left|\frac{\partial\Psi_d}{\partial\beta} I_a \cos(\beta)\right|\right]. \end{aligned} \tag{33}$$

In order to study the relationship between the terms $|I_a^2 \sin 2\beta\partial L_q/(2\partial\beta)|$, $|L_d I_a^2 \cos^2(\beta)|$, and $|I_a \cos(\beta)\partial\Psi_d/\partial\beta|$, their variations with $\beta$ when $I_a = 77$ A obtained from the nonlinear IPMSM model are shown in Fig. 2.

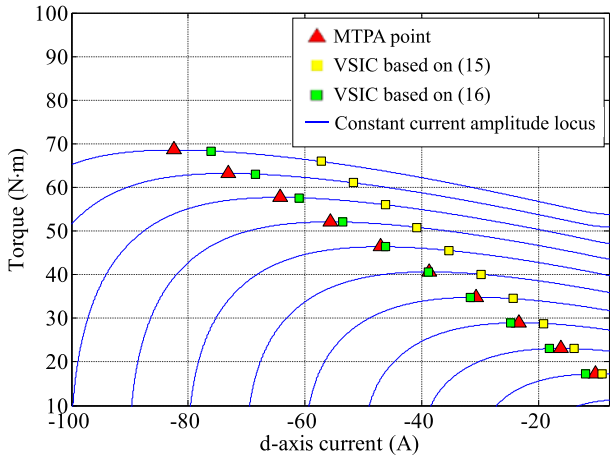


Fig. 3. MTPA points and the MTPA tracking simulation results of virtual signal injection control based on (15) and (16).

As can be seen from Fig. 2, $|I_a^2 \sin 2\beta\partial L_q/(2\partial\beta)|$ increases monotonically when $\beta < 45°$ while the terms $|L_d I_a^2 \cos^2(\beta)|$ and $|I_a \cos(\beta)\partial\Psi_d/\partial\beta|$ decrease. Moreover, $|L_d I_a^2 \cos^2(\beta)|$ and $|I_a \cos(\beta)\partial\Psi_d/\partial\beta|$ are with opposite signs in (32) but of similar magnitudes since $\partial\Psi_m/\partial\beta$ and $i_d\partial L_d/\partial\beta$ in (29) are relatively small. Therefore, $error_1$ is dominated by $|I_a^2 \sin 2\beta\partial L_q/(2\partial\beta)|$. Because the value of $|I_a^2 \sin 2\beta\partial L_q/(2\partial\beta)|$ is dependent on $I_a$ and $\beta$, $error_1$ will become significant when the resultant torque and the optimal current angle are relatively large. For the machine whose MTPA current angle is between 20° and 45°, i.e., IPMSM, the term $|I_a^2 \sin 2\beta\partial L_q/(2\partial\beta)|$ and the term $|I_a \cos(\beta)\partial\Psi_d/\partial\beta|$ in (33) can partly cancel each other. Therefore, the virtual signal injection based on (16) may have higher accuracy than that based on (15). However, for the machines with small reluctance torque, i.e., surface mounted permanent magnet machines, where $\beta$ angle for MTPA operation is close to zero, the virtual signal injection based on (15) is preferred because $|I_a^2 \sin 2\beta\partial L_q/(2\partial\beta)|$ is small around $\beta = 0$. In such cases, $L_d$ in (15) can be set to its nominal value or obtained from a look-up table. In real applications, whether (15) or (16) should be adopted can be determined by comparing the MTPA tracking accuracy at high torque demand.

To verify the above conclusions, the MTPA tracking results of the virtual signal injections based on (16) and (15) are shown in Fig. 3. As can be seen, the MTPA points tracked by the virtual signal injection control (VSIC) based on (16) reported in [1] have higher accuracy than (15) since $|I_a^2 \sin 2\beta\partial L_q/(2\partial\beta)|$ and $|I_a \cos(\beta)\partial\Psi_d/\partial\beta|$ in (33) can cancel each other partly.

The variations of $error_1$, $error_2$, and $\partial T_e/\partial\beta$ with $\beta$ when $I_a = 77$ A are compared in Fig. 4. As can be seen, $error_1$ and $error_2$ are not negligible compared with $\partial T_e/\partial\beta$. As the current angle increases, $error_1$ keeps increasing and is always greater than zero. While $error_2$ varies from negative to positive. When $\beta < 22°$, $|error_2| > |error_1|$, the virtual signal injection based on (15) has relatively small error. If $\beta > 22°$ and $|error_2| < |error_1|$, the virtual signal injection based on (16) yields better results due to the $|I_a^2 \sin 2\beta\partial L_q/(2\partial\beta)|$ and $|I_a \cos(\beta)\partial\Psi_d/\partial\beta|$ in (33) can partly cancel each other.

These characteristics are, indeed, validated by experiments reported in [1]. While the simulations and experiments are performed against a specific prototype IPMSM, the analysis described previously is applicable to any IPMSM. It should also be noted that since torque variation with current angle in the vicinity of the MTPA point is relatively small, small deviation of the *d*-axis current from the MTPA

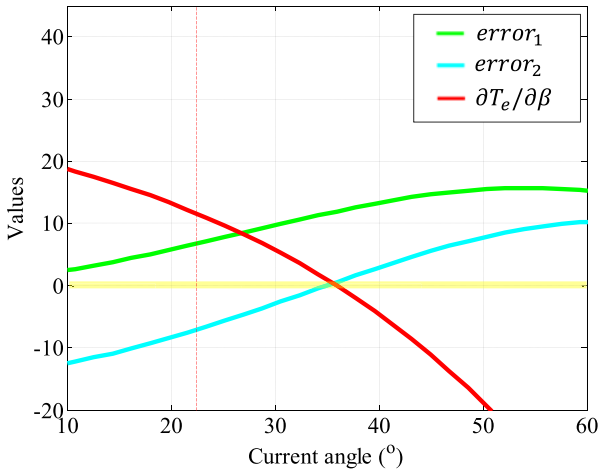


Fig. 4. Comparison of $error_1$, $error_2$, and $|\partial T_e/\partial\beta|$ when $I_a = 77$ A.

would not cause a significant reduction in the torque, as can be seen in Fig. 3. In a practical application, it would be useful to analyze the nonlinear characteristics of the machine and to select an appropriate formula for the VSIC-based MTPA tracking and whether (15) or (16) should be adopted can be determined by comparing MTPA tracking accuracy at high torque demand.

## II. Conclusion

MTPA tracking accuracy of the VSIC scheme for IPMSMs has been analyzed. It has been shown that due to parameter variations with stator currents in IPMSMs, any technique that determines MTPA operating condition by assuming piecewise constant parameters will result in tracking errors. These include online calculation of optimal $d$-axis current reference using machine parameters obtained from look-up tables or through online parameter estimations. The virtual signal injection control can be realized based on (15) or (16). For IPMSMs with relatively low reluctance torque contribution, including surface-mounted permanent magnet machines, the VSIC based on (15) would yield more accurate results. For the IPMSMs with relatively large reluctance torque contribution, the VSIC based on (16) may give the better tracking accuracy. In real applications, whether (15) or (16) should be adopted can be determined by comparing MTPA tracking accuracy at high torque demand. These findings provide fundamental understanding and clarification for achieving MTPA operation of IPMSM drives.

## References

[1] T. Sun, J. Wang, and X. Chen, "Maximum torque per ampere (MTPA) control for interior permanent magnet synchronous machine drives based on virtual signal injection," *IEEE Trans. Power Electron.*, vol. 30, no. 9, pp. 5036–5045, Sep. 2015.

[2] J. Lee, K. Nam, S. Choi, and S. Kwon, "Loss-minimizing control of PMSM with the use of polynomial approximations," *IEEE Trans. Power Electron.*, vol. 24, no. 4, pp. 1071–1082, Apr. 2009.

[3] Y. Jeong, S.-K. Sul, S. Hiti, and K. M. Rahman, "Online minimum-copper-loss control of an interior permanent-magnet synchronous machine for automotive applications," *IEEE Trans. Ind. Appl.*, vol. 42, no. 5, pp. 1222–1229, Sep./Oct. 2006.

[4] S.-Y. Jung, J. Hong, and K. Nam, "Current minimizing torque control of the IPMSM using Ferrari's method," *IEEE Trans. Power Electron.*, vol. 28, no. 12, pp. 5603–5617, Dec. 2013.

[5] Y. A.-R. I. Mohamed and T. K. Lee, "Adaptive self-tuning MTPA vector controller for IPMSM drive system," *IEEE Trans. Energy Convers.*, vol. 21, no. 3, pp. 636–644, Sep. 2006.

[6] G. Schoonhoven and M. N. Uddin, "MTPA and FW based robust nonlinear speed control of IPMSM drive using Lyapunov stability criterion," *IEEE Trans. Ind. Appl.*, vol. 52, no. 5, pp. 4365–4374, Sep./Oct. 2016.

[7] M. N. Uddin and M. M. I. Chy, "Online Parameter-estimation-based Speed Control of PM AC Motor Drive in Flux-weakening Region," *IEEE Trans. Ind. Appl.*, vol. 44, no. 5, pp. 1486–1494, 2008.

[8] D. Q. Dang, M. S. Rafaq, H. H. Choi, and J.-W. Jung, "Online Parameter Estimation Technique for Adaptive Control Applications of Interior PM Synchronous Motor Drives," *IEEE Trans. Ind. Electron.*, vol. 63, no. 3, pp. 1438–1449, Sep./Oct. 2016.

[9] A. Shinohara, Y. Inoue, S. Morimoto, and M. Sanada, "Direct calculation method of reference flux linkage for maximum torque per ampere control in DTC-based IPMSM Drives," *IEEE Trans. Power Electron.*, vol. 32, no. 3, pp. 2114–2122, Mar. 2017.